2009

Thin Wire Nucleate Boiling of Water in Sustained Microgravity

Justin P. Koeln

Heng Ban
Utah State University - Faculty Advisor

JR Dennison
Utah State University

Thin Wire Nucleate Boiling of Water in Sustained Microgravity

Justin P. Koeln[1]

Utah State University

Advisors: Dr. Heng Ban[2] *and J. R. Dennison*[3]

Abstract – **The advancement of small satellite technology relies on the development of effective thermal management systems that can be made smaller, safer, and more robust. This paper presents the results and analysis of a nucleate boiling experiment in sustained microgravity aboard the Space Shuttle Endeavor (STS-108). Bubble growth and departure were observed from a single and a braid of three 0.16 mm diameter and 80 mm long nickel-chromium resistive wires. Analysis showed that the braided wire provides a unique surface configuration to enhance the onset of boiling. The braid of wires was also observed to produce several bubble explosions; this is the first observation of such phenomenon under microgravity conditions. Bubble explosions are being researched on Earth due to their ability to remove large amounts of heat. Large spherical bubbles enclosing the wire were not observed, in contrast to many previous thin wire microgravity boiling experiments which often lead to the burnout of the heating element in microgravity. Measured bubble propagation was in good agreement with several prediction models based on drag forces. The effects of bubble formation, departure, and propagation on the temperature gradients in the fluid were analyzed. Applications for the development of microgravity heat transfer systems based on boiling mechanisms are discussed, along with the potential for further research utilizing small satellite technology.**

Nomenclature

a	=	drag coefficient prediction constant
A	=	bubble cross-sectional area
A_c	=	contact area
C_d	=	coefficient of drag
D	=	bubble diameter
F_b	=	buoyant force
F_D	=	departure force
F_d	=	drag force
F_i	=	inertia force
F_p	=	pressure force
F_R	=	resistant force
F_s	=	surface tension force
g	=	gravitational acceleration
g_0	=	gravitational acceleration on Earth
m	=	bubble mass
Mo	=	Morton number
q''	=	heat flux
R	=	bubble radius
R_0	=	wire radius
Re	=	Reynolds number
t	=	time
v	=	bubble velocity
We	=	Weber number
x	=	distance from wire
α	=	thermal diffusivity
β	=	contact angle
μ_l	=	viscosity of water
σ	=	surface tension
ρ_l	=	density of water
ρ_v	=	density of water vapor

I. Introduction

As technology advances toward the exploration and development of space, we require safe, efficient, and cost effective thermal management systems utilizing phase change mechanisms. Nucleate boiling is a well known, highly efficient mode of heat transfer; however, the absence of free convection due to lack of gravity reduces the convective heat transfer on orbit, resulting in more localized heating and larger thermal gradients. Microgravity experimentation is needed to provide the basis for the fundamental understanding of the behavior of boiling in space before thermal management, fluid handling and control, and power systems based on phase change can be designed for use on satellites and deep space probes.

With the development of more robust thermal management systems, small satellite technology can become more capable, more compact and more reliable. Understanding the conditions and dynamics of nucleate boiling in order to effectively harness its heat transfer capabilities is vital to the development of these more productive and cost effective small satellites.

Small satellite technology can also be used to study nucleate boiling. The sustained microgravity and lower costs of small satellite technology provides

1 – Undergraduate, Mechanical and Aerospace Engineering
2 – Associate Professor, Mechanical and Aerospace Engineering
3 – Professor, Physics

an ideal platform for boiling or phase change heat transfer research.

This paper presents the results and analysis of a thin wire nucleate boiling of water experiment performed on orbit aboard Space Shuttle Endeavor (STS-108). The residual gravity level on the Space Shuttle is negligible, reported to be $10^{-3}g_0$-$10^{-5}g_0$.[1,2] The experiment showed that bubble ejection from the heating element is possible even without buoyancy. Due to the heavily subcooled working fluid, bubble explosions in microgravity were observed; this has not been previously reported in the literature. The braid of three nichrome wires proved to effectively enhance the onset of boiling due to its unique configuration. Based on visual and thermal data from the experiment, correlations of the trajectory of a bubble after departing the wire were developed with numerical predictions based on drag dynamics. Thermal simulations were compared to the experimental temperature measurements to understand the effects of bubble propagation on heat transfer.

II. Background

A. Nucleate Pool Boiling

Different modes of boiling occur based on the excess temperature and the heat flux into the fluid. The excess temperature is the difference between the temperature of the heating surface and the liquid's saturation temperature, at which the liquid boils for a corresponding saturation pressure. Figure 1 shows the relationship between excess temperature and the surface heat flux as well as different boiling regimes for water at 1 atm.[3] Nucleate boiling can be further divided into two distinct modes: isolated bubbles and jets and columns. The low end of the nucleate boiling regime has relatively few nucleation sites, therefore producing distinct isolated bubbles. The upper end of the nucleate boiling regime has many nucleation sites in proximity, causing bubble interference and coalescence, producing jets and columns of vapor.

This study observes formation and departure of isolated bubbles under heavily subcooled conditions and, therefore, only deals with the segment of the boiling regime where the excess temperature is between 5°C and 10°C. Many terrestrial engineering devices take advantage of the nucleate boiling regime due to the high heat transfer rates and convection coefficients associated with small values of excess temperature. The formation, growth, departure, and travel history of bubbles control the heat transfer coefficient of boiling; therefore, this study intends to provide a detailed description of the bubble growth, departure and travel history under microgravity.

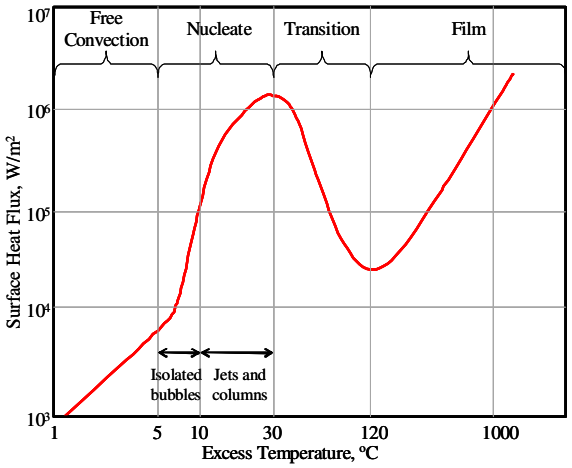

Figure 1. Boiling regimes for water at 1 atm, taken from Incropera.[3]

There also exists a significant difference between 1-g and 0-g boiling: the entire liquid in 1-g boiling is generally at saturation temperature, whereas in 0-g, the lack of natural convection causes the liquid to only be at saturation temperature in proximity to the heating surface. Away from the heating surface, the water can be significantly below saturation temperature. In previous experimentation, 0-g boiling developed a large coalescing bubble that engulfed the heating element, preventing heat transfer and causing overheating and burnout of the heating element.

B. Previous Research on Nucleate Boiling in Microgravity

Terrestrial based experimentation has developed an extensive database and understanding of the forces and factors that influence nucleate boiling dynamics. Studies have verified theoretical calculations of inertia, buoyancy, surface tension, and drag as a bubble nucleates and travels through a fluid as well as the bubble's diameter and contact angle upon departure. Without the dominant force of buoyancy, bubble dynamics and heat transfer differ greatly in microgravity. The inaccessibility of on-orbit experimentation is the leading reason for the lack of understanding of boiling dynamics in microgravity. In order to reduce costs, the majority of microgravity boiling research has been preformed utilizing microgravity simulators such as drop towers and NASA's KC-135A.

Siegel and Usiskin[4] performed pool boiling studies using a 2.5 meter drop tower capable of reducing acceleration to 1.4% g_o. Using a horizontal 0.5 mm wire, they observed enhanced heat transfer in the lower nucleate boiling regime for water and alcohol, but no enhancement for a 60% sucrose

solution. The heat transfer enhancement was also noticed to decrease with an increase in heat flux.

Tokura et al.[5] boiled methanol using thin platinum wires of 0.1 and 0.05 mm diameter. The Japan Microgravity Center (JAMIC) dropshaft used for the experiment produces less than 0.1% g_o for ~10 seconds. The heat transfer coefficient was observed to be approximately that of similar boiling in normal gravity. Two distinct bubble dynamics were observed. Under low heat flux conditions, small bubbles sprung from the wire and quasi-steady-state nucleate boiling was obtained. Under higher heat flux conditions, lateral coalescence of bubbles along the wire formed a large spherical bubble that enclosed the wire causing it to overheat, leading those authors to conclude that steady state boiling could not be achieved at high heat flux in microgravity.

Motoya et al.[6] obtained similar results to those of Tokura using the same JAMIC facility. Water was boiled with a 0.2 mm diameter platinum wire. Since water has a higher boiling point than methanol, a higher heat flux was needed and a large coalescing bubble formed, causing burnout of the heating element.

Zhao et al.[7] noticed enhancement in heat transfer when boiling in the lower nucleate boiling regime for R113 fluid utilizing the Drop Tower Beijing which provides 3.6 seconds of microgravity. Bubble departure diameter was not observed to be affected by variations in gravitation. Lateral oscillations were always observed which often led to coalescence between bubbles and detachment. The coalesced bubbles did not always detach and enclosed the wire creating a hot spot. Similar drop tower experiments were performed by Sitter.[8]

Parabolic flights, sounding rockets and orbital flights have also been used to simulate microgravity for nucleate boiling experimentation. Straub[9,10,11] and colleagues have experimented extensively with the pool boiling of refrigerants (R113, R12, R134a) using wires of 0.05, 0.2 and 8 mm diameter. In these experiments, heat transfer was found to be only slightly enhanced or was unaffected by microgravity conditions. Departure diameters four times that found in gravity were observed in the KC-135a experiments. Other experiments have also been performed using parabolic flights (Shatto and Peterson[12], Di Marco and Grassi[13]), sounding rockets (Di Marco et al.[14]), and the Space Shuttle (Steinbichler et al.[15], Hasan et al.[16]).

Zhao et al.[1,2] performed one of the few on-orbit experiments using the 22nd Chinese recoverable satellite with residual gravity between 0.001% and 0.1% g_o. They studied the boiling of subcooled R113 at 0.1 MPa using a 0.06 mm diameter platinum wire 30 mm in length. Several conclusions were obtained from this study, the first being that the onset temperature of boiling is independent of gravity. Heat transfer was also noticed to be slightly enhanced in microgravity. The authors were able draw several conclusions about the behavior of bubbles based on size and resulting departure forces. Small bubbles, less than 0.3 mm diameter, continuously formed on the wire and grew until slowly departing the wire. Larger bubbles, 3.5 – 6.6 mm diameter, oscillated on the wire and coalesced with adjacent bubbles. The largest bubbles, greater than 10 mm, stayed on the wire and grew by swallowing adjacent bubbles. The latter two types of bubbles were only observed in microgravity.

From the conclusions drawn from pervious experimentation, the results appear to be contradictory. This is due to the fact that boiling behavior in microgravity is heavily dependent on factors such as working fluid, heating surface, heat flux, level of subcooling, experiment duration, level of microgravity, and experimental apparatus. Due to the dependence on these factors, results can only be drawn for individual experimental systems and often cannot be used to predict boiling behavior for other systems. Therefore, there is a need for more experimentation in order to develop a fundamental understanding of the phenomena.

The majority of these experiments used refrigerants for the working fluid, due in part to their relevance to space system applications but also due to their low boiling point. The drop towers and NASA's KC-135A provide only short durations of microgravity. Therefore, the working fluid must boil within several seconds of applied power which is typically not feasible with water. However, sustained microgravity experimentation utilizing small satellite technology, as demonstrated by Zhao et al.,[1,2] with water is vital to the exploration and development of space.

The current study observed the boiling of water using a single straight 0.16 mm diameter nichrome wire and a braid of three similar wires. This experiment is unique in the use of a braid of wires to understand the effects of surface characteristic on the onset time of boiling and the enhancement of bubble generation. Also, this experiment was performed under sustained microgravity providing a run time of 35 minutes for each heating element and used heavily subcooled water and relatively low heat flux in the nucleate boiling regime. Hundreds of bubbles were produced during the experiment, permitting results not presented in the previous literature.

III. Objectives

The research was performed with the following specific objectives:

1) Observe the nucleate boiling from single and braided thin heating wires in space,
2) Obtain size, position, velocity, and acceleration data from visual recordings of the nucleate boiling process in microgravity,
3) Examine effects of bubble generation and motion on heat transfer utilizing experimental thermal measurement and conduction modeling,
4) Verify drag force equations to analytically predict the propagation of bubbles after departing the wire, and
5) Determine the forces on a bubble as it grows on the wire to predict departure diameters.

IV. Theory

A. Forces on a Bubble While Growing on the Heating Element

The forces acting on a bubble forming on a thin wire can be divided into departure forces, F_D, and resistant forces, F_R. If the departure force is greater than the resistant force, the bubble departs the wire (Equation 1). The departure forces include the inertia force, F_i, the pressure force, F_p, and the buoyant force, F_b. The resistant forces are the drag force, F_d, and the surface tension force, F_s. Figure 2 shows theses forces acting on a bubble.

$$F = F_D - F_R = (F_i + F_p + F_b) - (F_d + F_s) \quad (1)$$

The inertia force results from the growth of the bubble putting the surrounding fluid in motion. Equation 2 shows the inertia force is equal to the mass of a sphere of liquid of the same radius as the bubble multiplied by the acceleration of the bubble radius.

$$F_i = -\frac{4}{3}\pi R^3 \rho_l \frac{d^2R}{dt^2} \quad (2)$$

The pressure force, Equation 3, results from the pressure difference inside the bubble and the surrounding fluid. The higher internal vapor pressure causes a force on the heating element creating a departure force.

$$F_p = \left(\frac{2\sigma}{R} + \frac{p_l R}{3}\frac{d^2R}{dt^2} + C_d \frac{p_l}{8}\left(\frac{dR}{dt}\right)^2 \right) A_c \quad (3)$$

The buoyancy force in Equation 4, results from the difference between the density of the liquid and the vapor. Even though gravity levels of $10^{-3}g_0$-$10^{-5}g_0$ are quite small, the resulting buoyancy force significantly affects the total force on the bubble.

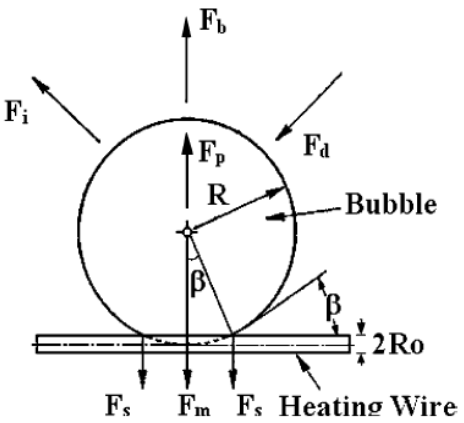

Figure 2. Departure and resistant forces on a growing bubble.[15]

$$F_b = \frac{4}{3}\pi R^3 (\rho_l - \rho_v) g \quad (4)$$

The drag force is the resistance of the fluid on the wall of the bubble as the radius increases (Equation 5).

$$F_d = C_d \frac{p_l}{2}\left(\frac{dR}{dt}\right)^2 A \quad (5)$$

The surface tension force, Equation 6, is the force of adhesion between the water surrounding the bubble and the heating element.

$$F_s = 4R_0 \sigma \sin^2\beta \quad (6)$$

Where the drag coefficient, C_d, and the contact area, A_c, are calculated with Equations 7 and 8, respectively.

$$C_d = 5{,}360\left(\frac{\rho_l R}{\mu_l}\frac{dR}{dt}\right)^{-0.79} \quad (7)$$

$$A_c = 4RR_0 \sin^2\beta \quad (8)$$

B. Drag Force on a Vapor Bubble After Departing the Heating Element

Once the bubble on the wire reaches a critical size by vapor accumulation or the coalescence of two adjacent bubbles, the bubble detaches from the wire. Upon departure from the heating surface, the bubble decelerates due to the drag force exerted by the quiescent water. Drag, F_d, is a function of the coefficient of drag, C_d, the density of the fluid, ρ_l, the cross-sectional area, A, and the velocity relative to the liquid, v, as shown in Equation 9.

$$F_d = -\frac{1}{2}\rho_l v^2 A C_d \tag{9}$$

Without buoyancy, the force balance from Newton's second law simply consists of the drag force and change in momentum of the bubble: thus,

$$F_d = \frac{d(mv)}{dt} \tag{10}$$

Classic bubble dynamics estimates the bubble mass as 11/16 of the mass of the fluid that would occupy the space of the bubble. This estimation, developed by Han and Griffith,[17] accounts for fluid carried with the bubbles during transit. Thus, assuming negligible phase change at the bubble's surface after leaving the wire, the force balance becomes as shown in Equation 11.

$$-\frac{1}{2}\rho_l v^2\left(\frac{\pi}{4}D^2\right)C_d = \frac{11}{16}\rho_l\left(\frac{1}{6}\pi D^3\right)\frac{dv}{dt} \tag{11}$$

Simplified, the equation becomes,

$$\frac{dv}{dt}v^{-2} = -\frac{12}{11}\frac{C_d}{D} \tag{12}$$

For a constant drag coefficient, the integration of Equation 12 is simple; however, as the bubble moves out towards colder water, the drag coefficient changes with time, thereby complicating the integration. For data processing, it is convenient to use the discretized velocity and displacement functions,

$$v_i = v_{i-1} - \frac{12}{11}v_{i-1}^2\frac{C_{d,i-1}}{D}\Delta t \tag{13}$$

$$x_i = x_{i-1} + v_i\Delta t \tag{14}$$

As seen from Equation 13, the predicted velocity is dependent on the drag coefficient and the diameter of the bubble. The bubble diameter remains fairly constant in the current study; however, as aforementioned, the drag coefficient varies due to the bubble moving into colder water. This is ultimately due to the temperature dependency of the viscosity of the water as shown in Figure 3a. The change in viscosity affects the Reynolds number, thereby affecting the drag coefficient. Figure 3b shows the drag coefficient versus Reynolds number for a solid sphere.

The drag on a vapor bubble is different due to the dynamic vapor-liquid boundary caused by vortexes in the interior of the bubble. Several models exist which attempt to numerically predict the drag coefficient for a bubble at various Reynolds numbers. Gorring and Katz[18] presented a number of correlations based on the function

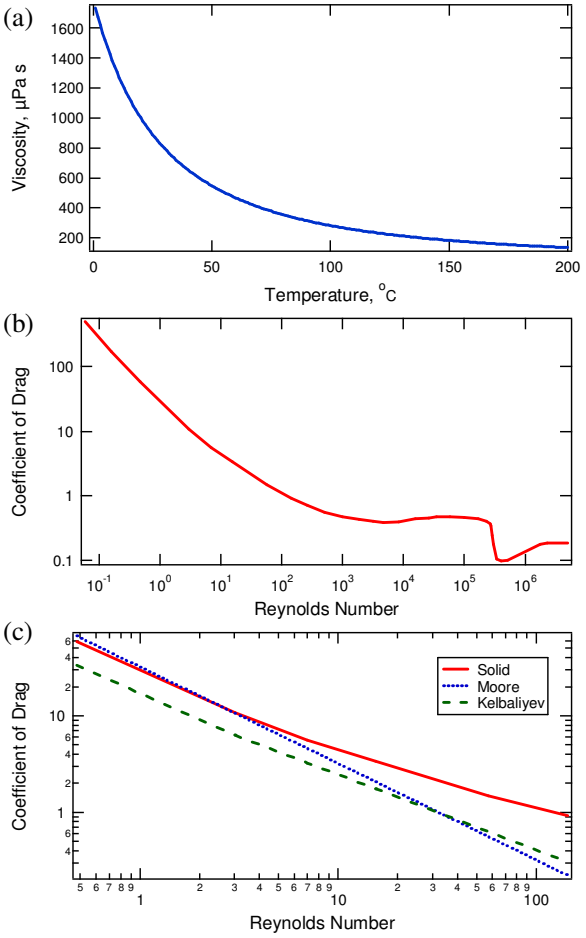

Figure 3. (a) Viscosity of water versus temperature. (b) Drag Coefficient versus Reynolds Number for a solid sphere. (c) Comparison between drag coefficient for a solid sphere and a bubble using Moore's and Kelbaliyev's methods.

$$C_d = \frac{a}{\mathrm{Re}} \tag{15}$$

where the constant a is dependent on the flow regime. Moore's relation assumes a = 32 and was used for this study within its limited range of Reynolds numbers. A more recent model by Kelbaliyev and Ceylan[19] integrates the full regime of $0.5 < \mathrm{Re} < 100$ as shown below:

$$C_d = \frac{16}{\mathrm{Re}}\left[1 + \left(\frac{\mathrm{Re}}{1.385}\right)^{12}\right]^{1/55} \tag{16}$$

Figure 3c show the difference between these two models and the standard model for a solid sphere.

Note that shape deformation of the bubble in this experiment can be considered negligible because it

meets the relation developed by Kelbaliyev and Ceylan[20]

$$\mathrm{Re}\,\mathrm{Mo}^{1/6} < 7 \qquad (17)$$

where $\mathrm{Mo} = 4/3C_d\mathrm{We}^3\mathrm{Re}^{-4}$ and $\mathrm{We} = (\rho_l v^2 D)/\sigma$. Predictions based on Moore's relation and the Kelbaliyev model were compared to the experimental data.

C. Heat Transfer

In microgravity, the lack of buoyancy prohibits convective heat transfer. Radiation is assumed negligible, leaving conduction as the only effective method of heat transfer. In order to understand the effects of bubble generation and propagation, thermal modeling was needed to determine the thermal gradients based solely on conduction. Equation 18 is an expression for the transient heat transfer.

$$\frac{1}{\alpha}\frac{\partial T}{\partial t} = \Delta T \qquad (18)$$

Using ANSYS, an engineering simulation software for finite element analysis, the temperature fields were modeled as a function of time. The model used an initial condition of T = 21 °C and boundary conditions of the chamber wall, T_{wall} = 21 °C and a heat flux of $q'' = 6.47\text{x}10^4$ W/m^2 for each of the three wires in the braided heating element, based on experimental conditions.

V. Experiment Description

The experiment consisted of a fluid chamber containing distilled water, the two heating elements, and six thermistors. The fluid chamber was comprised of five Lexan walls and one Viton rubber wall to allow for expansion in the case of sub-freezing temperatures during stowage. The heating elements were two nichrome wires; one a braid of three strands and the other a single strand. Six YSI 441107 Teflon-encapsulated thermistors were positioned at various distances from the heating elements. A CCD camera visually recorded the boiling and was digitized at 15 frames per second and 720 by 540 pixel resolution. The fluid chamber and schematic are shown in Figure 4 and Figure 5, respectively. The braided heating element was powered by 7 volts for 35 minutes using 40 lead X-cell batteries, generating a heat flux of $6.47\text{x}10^4$ W/m^2 on the surface. After the braided wire was turned off the boiling chamber was able to cool for one hour. The single wire was powered afterwards.

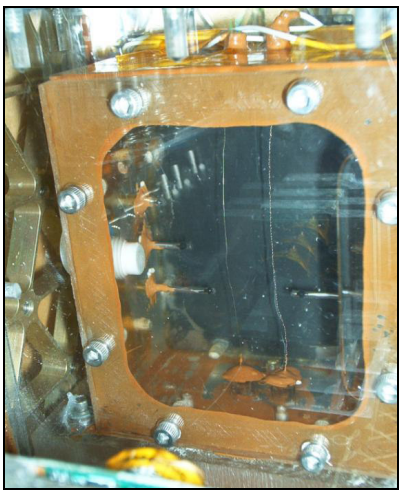

Figure 4. Front face of STS-108 experimental fluid chamber.

VI. Results and Analysis

A. Bubble Explosion

The 35 minute experimental run time allowed for an extensive duration of boiling, providing an unmatched observation opportunity not possible in previous experiments with restricted run times. At the onset of boiling, several bubble explosions, often referred to as bubble collapse or microbubble emission boiling (MEB), were observed (Figure 6). This phenomenon was first observed in 1986 by Inada et al.[21] and further research has shown that MEB can remove up to 14.41 MW/m^2 at a mass flux (of phase change) of 883.8 kg/m^{2}s, proving to be a promising method for the cooling of microelectronic chips.[22] This phenomenon occurs where coalesced bubbles generated on the heated surface at high heat flux were broken into many microbubbles after contacting with the surrounding liquid at a high degree of subcooling.[22] However, the physical understanding and mathematical description of the bubble explosion phenomenon are still to be developed. Insufficient subcooling is probably why other microgravity boiling experiments have not

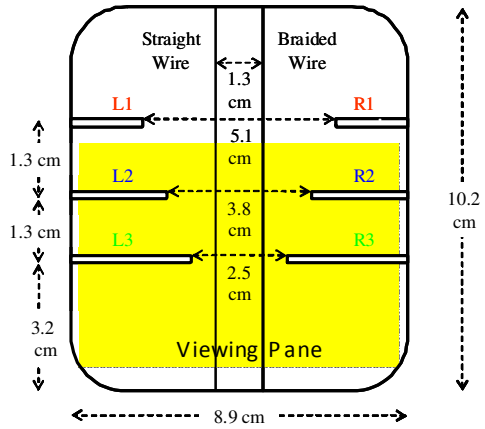

Figure 5. Chamber schematic.

observed this effect. Due to the constrained run times, the working fluid in those experiments could not be at the necessary level of subcooling. Shoji and Yoshihara[23] discovered MEB occurs with subcooling greater than 40K on Earth. The absence of convection in space, creates the greater thermal gradient required for MEB using less heat flux. Figure 7 shows the temperature from the ANSYS model at varying distances from the center of the braid of wires after 2 minutes of power. Notice that the temperature close to the surface of the wire is approximately 105°C while the temperature 1.8 mm (diameter of exploded bubble) from the wire is less than 50°C. This difference in temperature probably creates the instability of the vapor-liquid boundary causing the bubble explosion and microbubble emission.

This paper reports the first observation of bubble explosion in microgravity, with a unique wire configuration. The corresponding surface heat flux, 6.47×10^4 W/m^2, is much lower than required for 1-g conditions. This phenomenon needs to be further studied for better fundamental understanding, and for the potential development of highly efficient heat transfer mechanisms for thermal management systems in terrestrial and space applications. The unique three-wire configuration and 0-g condition provides an important tool for the investigation of the bubble explosion and microbubble emission phenomenon.

B. Bubble Size and Growth

After 2 minutes of power, 18 bubbles were observed in the visible section of the fluid chamber, which is approximately the middle third of the heating elements. Their measured diameters had an average of 0.8 mm. There was a significant increase in visible bubbles between 2 minutes and 4 minutes; however, there was not a significant increase in average bubble diameter. From 4 to 10 minutes, the number of bubbles remained fairly constant, but the average diameter constantly increased. After 10 minutes of power, the number and size of bubbles made the observation and measurement of individual bubbles increasingly difficult.

Bubble departure rate was also observed to vary with time. Within the first few minutes of power, many small individual bubbles departed the wire. Between 5 and 20 minutes, coalescence between adjacent bubbles was noticed which rarely caused the departure of the coalesce bubble. After 20 minutes, thousands of small (0.1-0.2 mm) bubbles departed the wire along with several very large bubbles (4-6 mm) filling the fluid chamber with bubbles of varying sizes. Most of the bubbles left the wires radially, but several departed at sharp angles often due to the

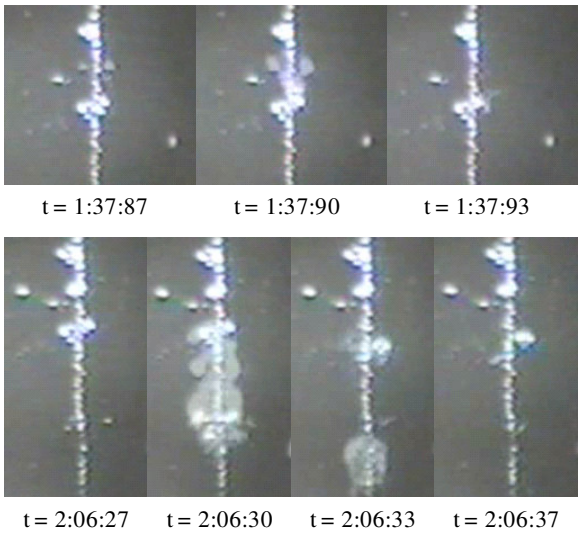

Figure 6. Photos of two bubble explosions (MEB).

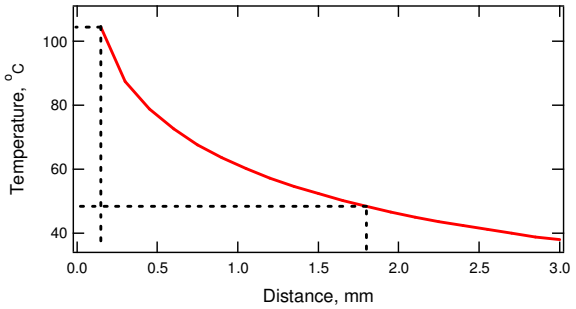

Figure 7. Temperature of fluid versus distance from center of braided wires from ANSYS modeling.

departure of adjacent bubbles. Most bubbles remained less than 25 mm away from the wire, but several propagated to the walls of the chamber.

There was an even spread of bubbles throughout the fluid chamber (Figure 11), indicating that the residual gravity had little effect on the growth or propagation of the bubbles during this experiment.

The growth of bubbles (Figure 8) is apparently heat transfer controlled, as opposed to inertia controlled, because the growth rate fits $R \propto t^{1/2}$. Given the accuracy of bubble diameter measurement is ±0.1 mm, the heat transfer controlled bubble growth curve fits most of the measured data points.

Bubble departure size was estimated using Equations (1) – (8). However, the result was not consistent with observations of departing size of 1.4-2 mm in the early stage, or 0.1-0.2 mm after 20 minutes. The difference in departure size at different times indicates the dependence on temperature and temperature gradient of the water. More detailed studies and analysis are needed to further understand the physical processes involved.

Also attributed to the long run time, observations on the total bubble volume with respect to time were obtained. Figure 9 shows the correlation between measured total volume of vapor present in the visible area of the fluid chamber with respect to time for the first 10 minutes of boiling. The R^2 value of 0.9974 reveals that constant heat flux produces a constant volume of vapor. This linear relation is expected to continue for the remainder of boiling indicating quasi-steady state nucleate boiling.

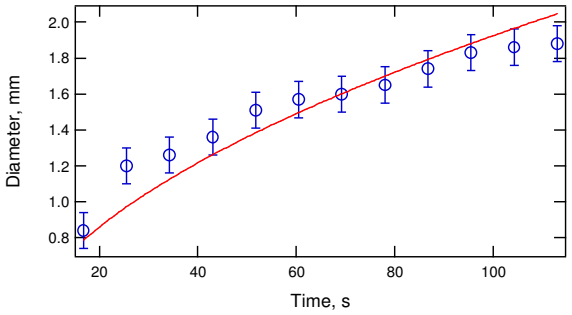

Figure 8. Measured bubble diameter with respect to time compared to predicted bubble growth.

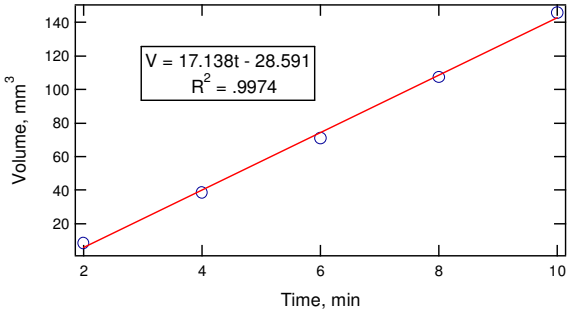

Figure 9. Total volume of vapor in fluid chamber versus time.

C. Temperature Profiles

Each thermistor measured the temperature of the water once per minute throughout the experiment. Figure 10 shows the temperature readings for 4 of the 6 thermistors. The data from L2 and R2 after the first 25 minutes was unreasonable. These thermistors may have experienced hardware failures. Convection from bubble movements may increase water temperature in a specific region. The L1, L3, R1, and R3 thermistors appear to have recorded reasonable data. The temperature of these four points did not change when bubbles first appeared on the braided wire in the first 9 minutes. At this time, the water adjacent to the wire is at saturation temperature while these four points, the closest being 12.7 mm from the wire, were still at about 21°C. When more bubbles began ejecting from the wire, a convective flow of water resulted and the thermistor temperatures started to rise at around 15-35 minutes. After the power was turned off, temperatures decreased due to cooling.

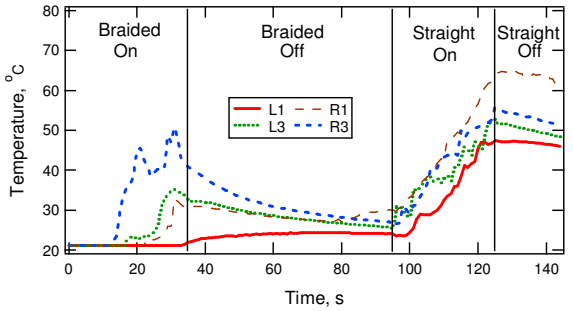

Figure 10. Thermistor readings over time.

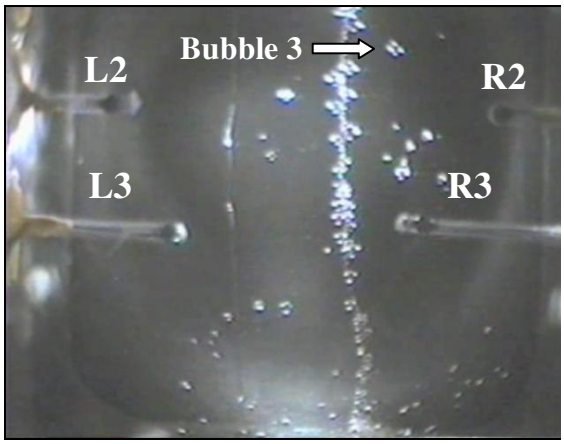

Figure 11. Photograph of nucleate boiling on a braided wire.

The power for the single wire was about three times that of the braided wire causing the temperature to increase almost immediately. Still, the recorded water temperature never surpassed 70°C, about 30°C below saturation temperature. This could only happen because of the absence of buoyancy-driven convective flow.

D. Thermal Model Predictions

Figure 12 shows the temperature distribution surrounding the three braided wires. Based on the ANSYS simulations, the interior region surrounded by the wires (red) reaches saturation temperature almost immediately after power is provided. The area between two wires (light blue), also reaches saturation temperature in about 120 seconds and is where the first bubbles nucleate. This quick achievement of saturation temperatures inside the three wires leads to the rapid generation of bubbles. Currently, surface boiling experiments utilize man-made cavities in the surface, which trap air, in order to generate bubbles. Without these cavities, the heater surface needs to be hot enough to heat the surrounding fluid to supersaturation temperatures. The braided wires produce bubbles without the need for cavities or large superheating of whole surfaces due to the concentration of heat flux in the center of the braid. Therefore, further research may prove a

braid of wires to be an effective form of bubble generation, which is an innovative approach not reported in the literature.

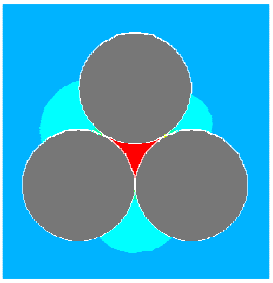

Figure 12. Temperature contours surrounding the heating wires at time t = 210s.

Figure 13 shows the measured temperature values during the first 35 minutes of the experiment when the braided wire was powered. Initially, the predicted temperatures exceed the measured data. At these times during the boiling, relatively few bubbles departed the wire. The bubbles on the wire thermally insulate the heating element, preventing heat from conducting through the fluid chamber. After approximately 15 minutes, more bubbles began to depart the wire causing the noticeable increase in measured temperature. The majority of the measured temperatures exceed the predicted model at some time from the increased heat transfer due to the bubbles carrying heated fluid away from the heating element, which was not included in the simulation.

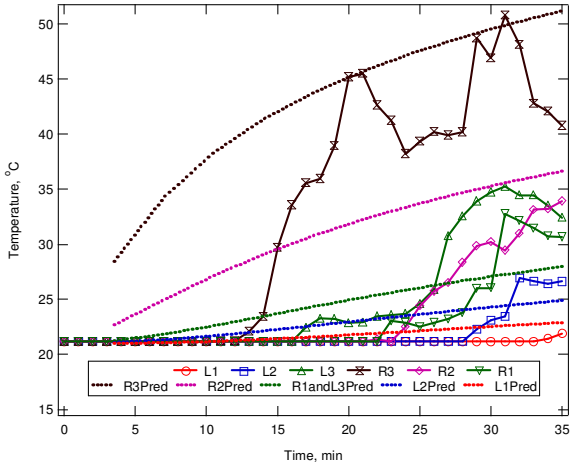

Figure 13. Measured and predicted temperatures over time.

E. Bubble Propagation

Pictures were extracted from the video at a rate of 10 frames per second for the first second after the separation of the bubble from the heating element for five bubbles. These five bubbles were chosen because they appeared to travel on the plane perpendicular to the camera. The size of the bubbles

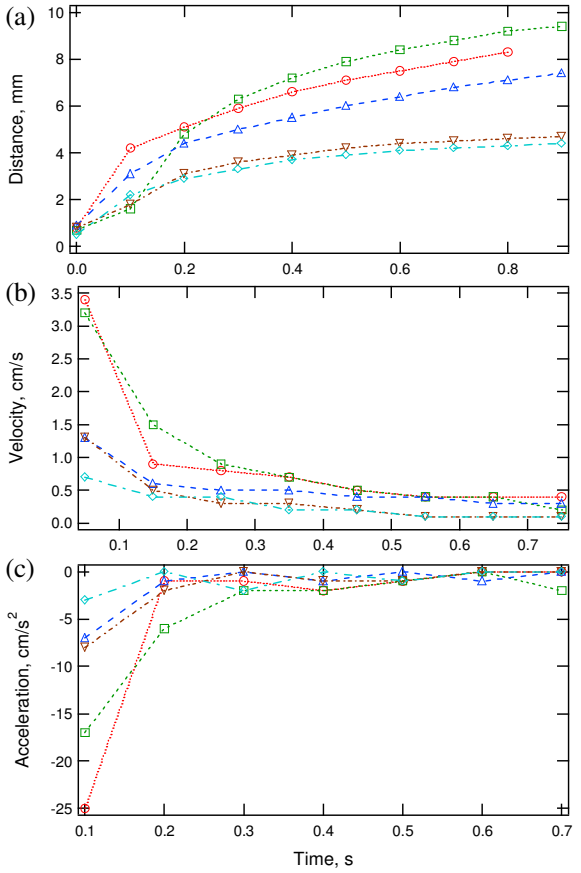

Figure 14. (a) Bubble center displacement from wire over time. (b) Bubble velocity after departure over time. (c) Bubble deceleration after departure over time due to drag.

was estimated to be about 1.5 mm, 1.5 mm, 2 mm, 1.6 mm and 1.4 mm for Bubbles 1, 2, 3, 4, and 5, respectively, with ±10% uncertainty due to resolution and lighting conditions. Figure 11 shows an example of a picture created from the video file. The bubble in the upper right corner is Bubble 3.

The position of the bubble over time was obtained by finding the pixel corresponding to the center of the bubble in each picture. Each pixel corresponds to approximately 0.1 mm physical length. Figure 14a shows the position of the five bubbles over time relative to the bubble leaving the wire.

The velocity (Figure 14b) of the bubbles was approximated using a first-order, center differencing approach for the differentiation.

$$v_{i+\frac{1}{2}} = \frac{x_{i+1} - x_i}{\Delta t} \qquad (19)$$

Due to the finite-differencing approach the number of data points decreases by one after each differentiation. The velocity of the bubble was greatest right after it broke free of the wire then,

quickly reduced to zero due to drag. The acceleration (Figure 14c) of the bubbles was also approximated using a first-order, center differencing, discretization approach.

$$\left(\frac{dv}{dt}\right)_{i+\frac{1}{2}} = \frac{v_{i+1} - v_i}{\Delta t} \qquad (20)$$

The predicted paths of a bubble after departing the thin wire determined using Moore's relation and the Kelbaliyev model are presented in Figure 15. It is evident that both models generally agree well with the experimental data, although Moore's model tends to yield more travelling distance than the Kelbaliyev model. Both prediction curves tended to plateau slightly quicker than the measured data for all five bubbles. For the empirically determined model inputs, Moore's relation initially overestimated the bubble position for approximately the first second after leaving the wire. Conversely, the Kelbaliyev model always under predicted the displacement of the bubble for all five bubbles. The prediction paths for bubbles with a lesser initial velocity appeared to fit the measured data most accurately.

F. Experimental Uncertainty

Bubble displacement was measured very accurately and, therefore, the experimental uncertainty resulted mainly from three parameters, bubble size, traveling direction, and time step. Figure 16a provides insight into the effects of measurement uncertainty of bubble size on the prediction methods for Bubble 1. The dashed lines represent a change in diameter of the bubble by one pixel. The effects of the diameter of the bubble are quite significant, yet due to the resolution of the video and poor lighting, bubble diameter had to be approximated to within ±0.1mm.

The motion of the bubble was measured in only two dimensions. Movement toward or away from the camera was not taken into account when measuring a bubble's distance from the wire because it could not be seen. Any motion in this third dimension would increase the bubble's measured distance, velocity and acceleration. Furthermore, while the added motion to or from the camera would add to the total dynamics of the bubble, this was not included in the numerical analysis of the model parameters.

The effects of the discrete position measurements are most apparent when the bubble has the highest velocity as soon as it breaks free of the wire. As the time step becomes smaller, the bubbles position and velocity upon departure is known more precisely. The time step was limited by digitization capabilities and frame rate of the CCD camera. With a time step of 0.1 seconds for velocities on the order of cm/s, a precise value for the initial velocity could not be

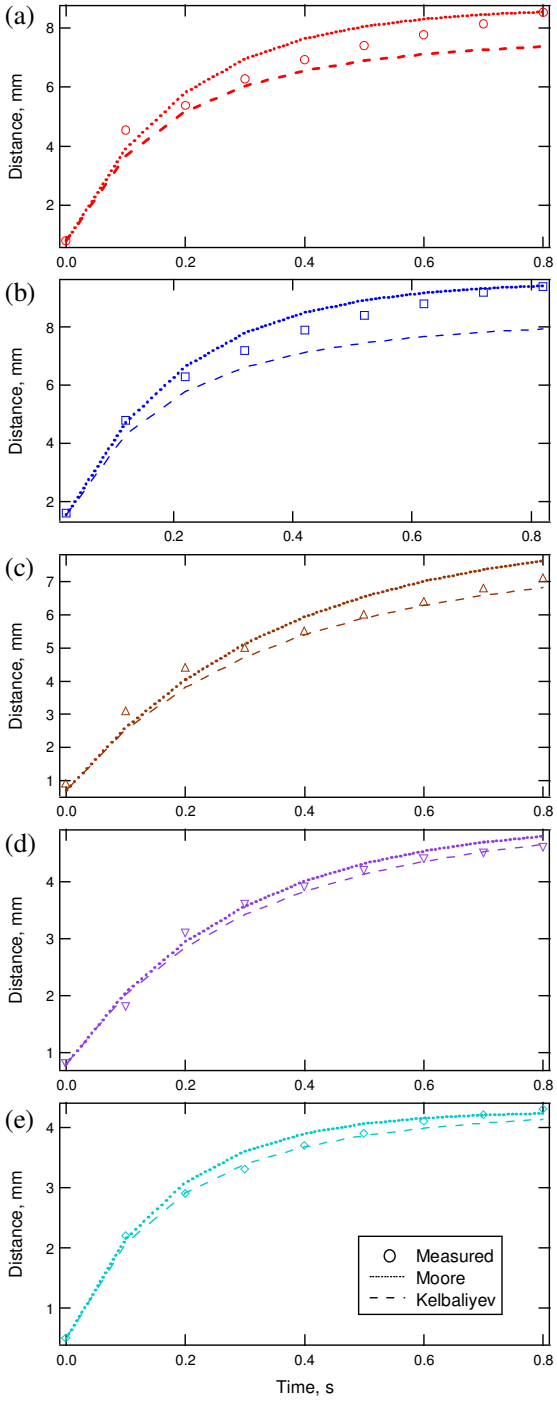

Figure 15. Measured and predicted displacement over time. (a) Bubble 1, D = 1.5mm (b) Bubble 2, D = 1.5mm (c) Bubble 3, D = 2.0 mm (d) Bubble 4, D = 1.8mm (e) Bubble 5, D = 1.4mm.

determined. Thus, the initial velocity for both prediction methods was estimated to best fit the measured data. Figure 16b shows the effects of the initial velocity on the prediction models. The dashed lines represent a 0.5 cm/s increase and decrease of the velocity of the bubble immediately after leaving

the wire. The low frame rate is expected to cause measured velocities to be less than true values. Therefore the upper dashed line could more accurately predict the propagation of the bubble. The Moore and Kelbaliyev prediction curves overlap under these uncertainty conditions and therefore are indistinguishable.

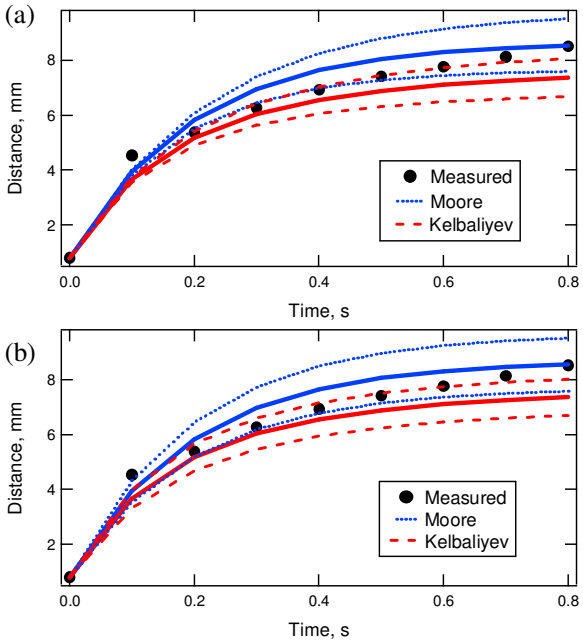

Figure 16. (a) Effects of bubble diameter on predicted displacement. (b) Effects of initial velocity on predicted displacement.

VII. Conclusions and Recommendations

Based on the results and analyses of the STS-108 experiment on nucleate boiling, several of which are first to be reported, the following conclusions can be made:

1) Bubble explosion and microbubble emission is possible in microgravity, and the phenomenon happened under low heat flux (6.47×10^4 W/m^2) and deep subcooling conditions. This paper is the first report of bubble explosion in microgravity.
2) Bubble radius growth is measured to be proportional to $t^{1/2}$, indicating the heat transfer controlled regime of bubble growth, and total vapor volume is linear with respect to time under constant heat flux.
3) A bubble can be ejected from a heated wire in the absence of gravity, due to the departure force overcoming the resistant forces at various bubble sizes.
4) The unique configuration of a braided wire heating element enhances bubble generation and conduction-induced thermal gradients within the water, which may lead to a new approach to bubble generation and heat transfer enhancement.
5) The temperature distribution without buoyancy is affected by bubble insulation on the heating wire, as well as water flow and heat transport caused by bubble propagation, resulting in a complex temperature field.
6) Moore's relation and the Kelbaliyev equation can be used to accurately model bubble drag and travel from a thin wire in zero gravity.

Further research is needed to understand the nucleate boiling process under various fluid, surface, and heat flux conditions under microgravity conditions in order to make satellite thermal management systems more efficient, safer, smaller and less costly.

Currently, Utah State University's Get Away Special (GAS) microgravity research team is in the design processes of developing a nucleate boiling experiment which will utilize a CubeSat as an experimental platform. The design incorporates better thermal monitoring and higher resolution video recording with a faster frame rate. Future research experiments should be designed in order to study the following characteristics of boiling.

1) Various heating elements of differing surface characteristics should be used to understand how the surface effects bubble generation, bubble growth, departure and heat transfer.
2) Different working fluids, including water, should be used to determine how the fluid properties effect boiling.
3) A range of subcooling needs to be analyzed in order to determine the effects on heat transfer.
4) A range of heat flux needs to be supplied to understand the conditions for small departing bubbles and large coalescing bubbles.

Further experiments need to be designed in order to obtain data on instantaneous provided power, time of power supplied to fluid, accurate bubble size, displacement, and direction, and temperatures in close proximity to the heating element.

Acknowledgments

The USU Get Away Special (GAS) team, particularly Jeffrey Duce, Arlynda Jorgensen and Ron Cefalo and his students, is acknowledged for designing and performing the experiment.

Jan Sojka, the GAS team advisor, and JR Dennison deserve special thanks for their leadership and support throughout the years.

Heng Ban and Jeffrey Boulware are acknowledged for their commitment to helping the author with the analysis and preparation of this paper.

Chunbo Zhang is acknowledged for his help modeling the temperature fields using ANSYS.

References

[1]Zhao, J. F., Liu, G., Wan, S. X., and Yan, N., "Bubble Dynamics in Nucleate Pool Boiling on Thin Wires in Microgravity," *Microgravity Science and Technology*, Vol. 20, 2008, pp. 81-89.

[2]Zhao, J. F., Wan, S. X., Liu, G., Yan, N. and Hu, W. R., "Subcooled Pool Boiling on Thin Wire in Microgravity," *Acta Astronautica*, Vol. 64, 2009, pp. 188-194.

[3]Incropera, F. P., Dewitt, D. P., Bergman, T. L., and Lavine, A. S., *Fundamentals of Heat and Mass Transfer*, 6th ed., John Wiley and Sons, New Jersey, 2007, pp. 621-626.

[4]Siegel, R., and Usiskin, C., "Photographic Study of Boiling in Absence of Gravity," *Journal of Heat Transfer, Trans. ASME*, Vol. 81C, 1959, pp. 230–236.

[5]Tokura, I., Hanaoka, Y., Suzuki, H., Hirata, H., and Yoneta, M., "Boiling Heat Transfer on Thin Wires in a Microgravity Field," *Proceedings of the ASME/JSME Thermal Eng. Conference*, Vol. 4, Maui, HI, 1995, pp. 555–560.

[6]Motoya, D., Haze, I., and Osakabe, M., "Effect of Fouling on Nucleate Pool Boiling in Microgravity and Earth Gravity," *ASME Heat Transfer Division*, Vol. 364–1, 1999, pp. 303–310.

[7]Zhao, J.F., Wan, S.X., Liu, G., and Hu, W.R., "Experimental Study on Subcooled Pool Boiling in Microgravity Utilizing Drop Tower," *Proceedings of the International Symposium on Multiphase Flow*, Beijing/NMLC., Xi'an, China, 2005.

[8]Sitter, J.S., Snyder, T.J., Chung, J.N., and Marston, P.L., "Acoustic Field Interaction with a Boiling System Under Terrestrial Gravity and Microgravity," *Journal of the Acoustical Society of America*, Vol. 104, 1998, pp. 2561–2569.

[9]Straub, J., "Boiling Heat Transfer and Bubble Dynamics in Microgravity," *Advances in Heat Transfer*, Vol. 35, 2001, pp. 57–172.

[10]Straub, J., and Micko, S., "Boiling on a Wire Under Microgravity Conditions – First Results from a Space Experiment," *Proceedings of Eurotherm Seminar No. 48*, Paderbom, Germany, 1996.

[11]Straub, J., Zell, M., and Vogel, B., "Boiling Under Microgravity Conditions," *Proceedings of the 1st European Symposium of Fluids in Space*, ESA SP-353, Ajaccio, France, 1992.

[12]Shatto, D.P., and Peterson, G.P., "Pool Boiling Critical Heat Flux in Reduced Gravity,". *Journal of Heat Transfer, Trans. ASME*, Vol. 121, 1999, pp. 865–873.

[13]Di Marco, P., and Grassi, W., "Motivation and Results of a Long-Term Research on Pool Boiling Heat Transfer in Low Gravity," *International Journal of Thermal Sciences*, Vol. 41, 2002, pp. 567–585.

[14]Di Marco, P., Grassi, W., and Trentavizi, F., "Pool Film Boiling Experiments on a Wire in Low Gravity: Preliminary Results," *Microgravity Transport Processes in Fluid, Thermal, Biological & Material Sciences*, edited by S. S. Sadhal, Vol . 26, Annals of the New York Academy of Sciences, 2001.

[15]Steinbichler, M., Micko, S., and Straub, J., "Nucleate Boiling Heat Transfer on Small Hemispherical Heaters and a Wire Under Microgravity," *Proceedings of the 11th International Heat Transfer Conference*, Vol. 2, Kyongju, Korea, 1998, pp. 539–544.

[16]Hasan, M. M., Lin, C. S., Knoll, R. H., Bentz, M. D., and Meserole, J.S., "Nucleate Pool Boiling in the Long Duration Low Gravity Environment of the Space Shuttle," NASA TM-105973, 1993.

[17]Han, C., and Griffith, P., "The Mechanism of Heat Transfer in Nucleate Pool Boiling," *International Journal of Heat and Mass Transfer*, Vol. 8, 1965, pp. 887-904.

[18]Gorring, R. L., and Katz, D. L., "Bubble Rise in a Packed Bed Saturated with Liquids", *American Institute of Chemical Engineers Journal*, Vol. 8, No. 1, 1962, pp. 123-126.

[19]Kelbaliyev, G., and Ceylan, K., "Development of New Empirical Equations for Estimation of Drag Coefficient, Shape Deformation, and Rising Velocity of Gas Bubbles or Liquid Drops," *Chem. Eng. Comm.*, Vol. 194, 2007, pp. 1623-1637.

[20]Kelbaliyev, G., and Ceylan, K., "Estimation of the Minimum Stable Drop Sizes, Break-up Frequencies, and Size Distributions in Turbulent Dispersions," *Journal of Dispersion Science and Technology*, Vol. 26, 2005, pp. 487-494.

[21]Inada, S., Miyasaka, Y., Sakamoto, S., Chandratilleke, G.R., "Liquid-solid contact state in subcooled pool transition boiling system," *J. Heat Transfer* Vol. 108, 1986, pp. 219–221.

[22]Wang, G., and Cheng, P., "Subcooled flow boiling and microbubble emission boiling phenomena in a partially heated microchannel," *International Journal of Heat and Mass Transfer*, Vol. 52, 2009, pp. 79-91.

[23]Shoji, M., Yoshihara, M., "Burnout heat flux of water on a thin wire," *Proceedings of 28th National Heat Transfer Symposium of Japan*, 1991, pp. 121–123.